ACS Sustainable Chemistry & Engineering

Research Article

pubs.acs.org/journal/ascecg

Current and Emerging Technologies for the Characterization of Nanomaterials

O. A. Sadik,*[,†] N. Du,[‡] V. Kariuki,[†] V. Okello,[†] and V. Bushlyar[†]

[†]Center for Advanced Sensors & Environmental Systems (CASE), Department of Chemistry, State University of New York − Binghamton, P.O. Box 6000, Binghamton, New York 13902-6000, United States

[‡]Laboratories and Scientific Services Directorate, Springfield Laboratory, U.S. Customs and Border Protection, U.S. Department of Homeland Security, 7501 Boston Blvd., Suite 113, Springfield, Virginia 22153, United States

ABSTRACT: This paper provides a survey of conventional and emerging techniques that are available for characterizing engineered nanoparticles in complex matrices. Techniques that were considered include microscopy (TEM, SEM, HRTEM, DLS, SNOM), chromatography (HDC, FFF), mass spectroscopy (ICP-MS, SEC-ICP/MS, MALDI, FFF-ICP-MS), sp-ICP-MS, and electrochemical techniques. A case study is presented from the authors' laboratories for the design of a portable nanoparticle analyzer based on tangential flow filtration and electrochemical detection (EC-TFF). EC-TFF is equipped with poly(amic) acid membrane filter electrodes (PMFE) arrays that perform multiple functions to capture, isolate, and detect (CID) engineered nanoparticles. The application of EC-TFF is presented for the characterization of engineered nanosilver in real-world samples. A size-dependent isolation of AgNPs was achieved at varying particle sizes with over 98.5% removal efficiency. PEC-TFF AA showed an excellent performance not only for isolation at subnanometer-sized ranges but also as a platform for detection of engineered nanoparticles at low ppb levels.

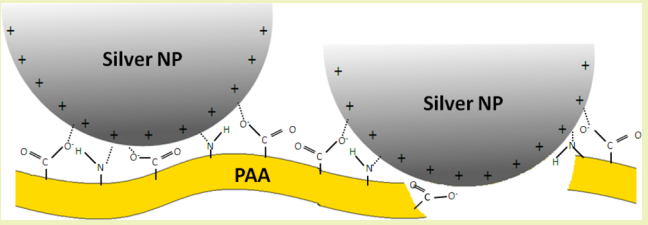

KEYWORDS: *Nanotools, Engineered nanoparticles, Electrochemistry, Tangential flow filtration*

INTRODUCTION

Engineered nanoparticles (ENPs) are ultrafine particles with one dimension between 1−100 nm[1]. Due to their small size, ENPs have very large surface areas relative to their weight, so they react quite differently from a bulk solid or dissolved material of the same composition. Consequently, their mechanical, magnetic, catalytic, electronic, optical, and biological features can easily be manipulated. ENPs are becoming valuable materials for applications in a broad range of fields, including food additives, cosmetics, biological samples, and pharmaceuticals, as well as in biocidal packaging, fuel cell technology, and electronics. However, the increase in the use of ENPs in consumer products has raised the concern over their environmental fate, potential toxicity, and overall risks to both environmental and human health.[2−4] For this reason, there is an urgent need to develop appropriate analytical tools and methods that are particularly useful for the evaluation of ENPs in complex matrices, consumer products, and personal electronics. The desirable tools are expected to be applicable or tunable to the specific properties of ENPs such as size distribution, particle number concentration, and mass concentration.[5,6] These methods must allow not only the determination of the NPs mass concentration but also the evaluation of their size, size distribution, and/or toxicity.

Extensive reviews of nanocharacterization tools have been published.[7−11] Numerous analytical techniques have been reported for the characterization of ENPs. In particular, the most commonly used techniques for obtaining the size distribution of ENPs and structural information include transmission electron microscopy (TEM), scanning electron microscopy (SEM), dynamic light scattering (DLS), atomic force microscopy to study morphology and topography, and NP tracking analysis and separation techniques. Others include capillary electrophoresis, hydrodynamic chromatography (HDC), ion mobility spectrometry, and field flow fractionation (FFF).[12] The investigation of the shape of ENPs (a relevant parameter in many applications) is readily achieved using TEM, SEM, DLS, atomic force microscopy, and FFF.[13] In addition, the chemical identification of major elements is possible using X-ray-based techniques, X-ray photoelectron spectroscopy (XPS), and energy dispersive X-ray spectroscopy. Thus, a rough elemental distribution of NPs is usually achieved by integrating these X-ray-based techniques with TEM/SEM or DLS information.[14]

Despite the existence of these characterization tools, there is no quantitative analytical tool for the measurement of ENPs in complex matrices. As discussed in this review, mass spectrometry has been coupled with chromatography, and the

Special Issue: Sustainable Nanotechnology 2013

Received: March 10, 2014
Revised: May 12, 2014
Published: May 20, 2014

   dx.doi.org/10.1021/sc500175v | *ACS Sustainable Chem. Eng.* 2014, 2, 1707−1716

resulting hyphenated techniques have been reported. These hyphenated techniques have enabled the prior removal of major interferences, and their performance characteristics are hereby evaluated on a case-by-case basis.[7]

MICROSCOPY TECHNIQUES

Microscopy is one of the most powerful techniques that can be used to determine the size, shape, and morphology of nanomaterials. Examples include electron and proton microscopy, atomic force microscopy (AFM), scanning probe microscopy, and scanning tunneling microscopy (STM), and each has unique advantages.[7] These techniques, when used, give little or no chemical information but provide excellent spatial resolution down to the atomic scale. However, some exceptions exist; for example, derivatized AFM tips can be used for chemical recognition.[15]

In TEM, when electrons are accelerated up to high energy levels and focused on a sample, changes to the electrons either through back scattering elastically or inelastically yields X-rays, auger electrons, or light. This interaction between sample and electron beams then gives rise to images. With a spatial resolution of 10 nm^{-1}, modern TEM is a very powerful technique for the characterization of nanoparticles. AFM, backed by its ability to provide real topographical images of surfaces, is used to measure surface properties such as frictional force on nanoscale, hardness of surfaces, surface charge distribution, surface magnetization, and yield stress.[10] STM is used for viewing the atomic surfaces. It uses a tunneling current to probe the density of the states of a material. It can achieve up to ~0.1 nm lateral resolution and 0.01 nm depth resolution.[10]

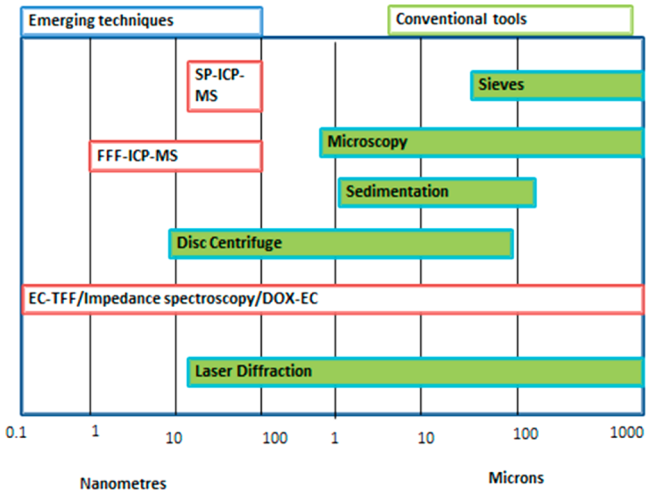

Figure 1. Survey of conventional and emerging tools for charactering engineered nanoparticles. SP-ICP-MS = single particle inductively coupled mass spectrometer. FFF-ICP-MS = fluid flow fractionation inductively coupled mass spectrometer. EC-TFF = electrochemical tangential fluid flow. DOX-EC = dissolved oxygen sensor coupled with electrochemical technique. DLS = dynamic light scattering.

Dynamic light scattering (DLS) and scanning electron microscopy (SEM) or transmission electron microscopy (TEM) are commonly used in *in vitro* cytotoxicity of silver nanoparticles (AgNPs). These generally enable nanoparticle size characterization once they have been dispersed in a buffer solution[16] or in a culture medium.[17] A DLS measurement of the hydrodynamic size of the particles in these complex media can be used to monitor the formation of nanoparticle agglomeration. Hassellöv et al.[18] and Calzolai et al.[19] have previously reviewed the limitations of DLS. Challenges have been largely attributed to the interpretation of data especially for polydispersed systems given the strong particle size dependence of the scattering intensity. SEM and TEM analyses allow us to study the changes in the shape of the nanoparticles along with the size distribution, although an accurate quantitative measurement requires counting and measuring a high number of particles,[18] which is time-consuming.

Cellular (*in vitro*) uptake of nanoparticles has also been examined in a number of studies[16,17,20,21] using two main techniques: Confocal laser scanning microscopy (CLS)[16,21] and TEM.[17,20] CLS microscopy measures the reflectance of the signal from silver nanoparticles or the fluorescence signal from the labeled nanoparticles using laser as an excitation source.[16]

HRTEM can be the best technique to identify crystalline structures as reported by Lan et al.[22] for CdS nanowires or for palladium nanorods as reported by Huang et al.[23] and graphene edges by Jia et al.[24] This technique does have some challenges. It is subject to artifacts caused by sample preparation. It also requires high vacuum and thin sample sections or particles of limited diameter to allow the electron beam to penetrate through the sample.[25]

SEM is one of the most versatile instruments available for the examination and analysis of the morphology and determination of chemical composition. SEM characterization usually occurs in vacuum, and sample preparation is achieved in solid state.[26] Besides yielding three-dimensional images, SEM has the ability to image large areas of samples and bulk materials such as thin films.[10] Toxicity of ZnO and Ag nanoparticles on bacterial cells has been examined using SEM by Sinha et al. This study validated the fact that the toxicity of the NPs depends primarily on the nature of the membrane and the interaction of the nanoparticles with the membrane. AFM, which has been used for imaging of samples in their native environment and to measure surface area of nanoparticles, is critical in nanotoxicity studies.[27] Scanning near-field optical microscopy (SNOM), an "optical relative" of AFM and STM, enables the study of a sample's optical properties with resolution far beyond the diffraction limit. SNOM combines excellent spectroscopic and temporal selectivity of classical optical microscopy with a lateral resolution reaching well into the sub-100 nm regime.[28] Sample fluorescence, light emission, transmission, scattering, etc. can be mapped with the spatial resolution down to tens of nanometers. Two main approaches to the near-field microscopy exist: (i) aperture type SNOM and (ii) apertureless techniques.[29] SNOM operates by illuminating a monochromatic plane wave from a laser into an optical fiber with a sharp tip such that only a very small aperture (diameter ≈ 50 nm) passes laser light. If brought close to the sample (within a few nm or into the optical near-field), this nanometer light source can be used to illuminate a spot on a sample that is considerably smaller than the optical diffraction limit. SNOM has a major limitation in its optical throughput when using very small apertures. This limits both the spatial resolution and the optical brightness of SNOM nano light sources. This limitation can be overcome by using aperture less near-field methods, such as tip-enhanced Raman scattering (TERS). A comprehensive review on SNOM and its applications has been written by Hecht et al.[28]

In summary, electron microscopy methods have been shown to provide powerful information,[30] but artifacts due to sample preparation, the high particle count required, and the lack of

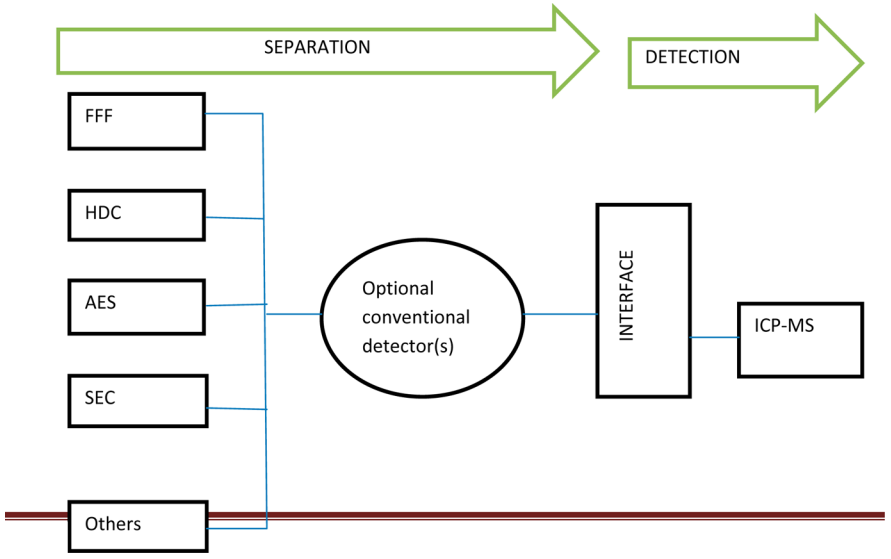

Figure 2. ICP-MS hyphenated techniques. FFF = field flow fractionation. HDC = chromatography. ICP-MS = inductively coupled plasma mass spectrometry. SEC = size exclusion chromatography. AES = auger electron spectroscopy.

suitability for high-throughput applications limit the application of these techniques in complex matrices.

Mass Spectrometry. There is a growing use of the mass spectrometry technique for the characterization of ENPs. This is because this technique offers invaluable elemental and molecular information on the composition, structure, and chemical state of NPs. In addition, the compatibility of MS with any type of sample can provide novel insights into the nature of NPs, while providing real time information due to its extremely high sensitivity and ease of coupling with other separation techniques.[31]

ICP-MS is an example of a coupled or hyphenated technique that is gaining importance as a tool for characterization of ENPs. In the ICP source, most elements are efficiently vaporized, atomized, and ionized (even from NPs) to provide a rapid and robust elemental chemical analysis. The outstanding features of ICP-MS have led to its broad application in nanoparticle characterization. These include robustness, high sensitivity (subparts-per-trillion level), wide dynamic range (up to nine of orders of magnitude), high selectivity, virtual matrix independence, etc. Also, ICP-MS requires simple calibration standards, and the use of isotope dilution techniques has proven very useful for an accurate elemental quantification.[32] Some illustrative applications for quantification and elemental analysis reported in the literature include the direct determination of metal oxide NPs such as Al_2O_3, TiO_2, CeO_2, and ZnO or metallic Ag and AuNPs in environmental samples.[33] Determination of metallic impurities in NPs has also been reported using ICP-MS. For example, a simultaneous determination of multielemental trace impurities in high-purity CeO_2, ZnO, SiO_2, and TiO_2 NPs after a microwave-assisted acid digestion has been conducted using high-resolution ICP-MS.[34]

Satoshi et al. used ICP-MS after microwave sample digestion in their investigation of the possibility of using AgNPs as a preservative in cosmetics.[35] They concluded that AgNP is safe to use as a preservative in cosmetic products because it does not penetrate into the skin except when there is a wound on the skin. Recently, when coupled with other techniques, ICP-MS has been used to probe real environmental samples (Figure 2). Hydrodynamic chromatography-inductively coupled mass spectrometry (HDC-ICP-MS) has been used for detecting and characterizing ENPs in aqueous matrices. Using this technique, Karen et al.[36] have investigated the nature and fate of AgNPs in an activated sludge. The particle-size distribution of the silver ENPs in the sludge was determined using TEM and HDC-ICP-MS. Size separation was achieved using a hydrodynamic chromatography column.

ENPs may consist of a core or a core/shell that is coated by ligands of different natures to confer more stability to the NP as a whole or to provide it with a specific functionality as shown in Figure 3. Such protective ligands may play a critical role in the

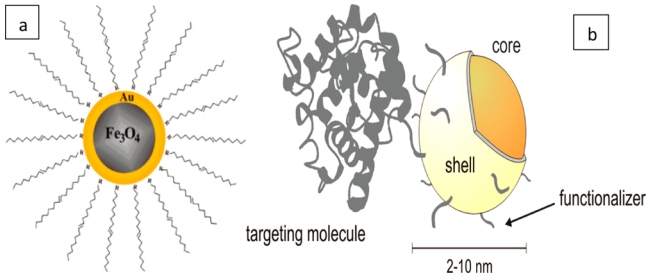

Figure 3. (a) Core–shell Fe_3O_4 and Au nanoparticle with an outmost organic shell encapsulation (R) CO_2H or $-NH_2$.[38] (b) Schematic representation of a functionalized core–shell quantum dot bound to a biomolecule.[39]

surface chemistry that governs any further functionalization processes used for subsequent bionanotechnological applications.[37] Molecular techniques such as electron spray ionization (ESI) and matrix-assisted laser desorption/ionization (MALDI) can provide such information. Molecular MS allows the core size to be estimated, the ligand layer to be characterized, and the molecular formula to be obtained. The analysis of thiolate-protected Au MPCs using MALDI has been well documented.[40] It is worth noting that the use of NPs to enhance MS tools has been proposed. NP-based substrates such as QDs, SiO_2, and TiO_2 NPs can be used in laser desorption/ionization MS techniques. Because NPs are excellent laser energy absorbing materials, they seem to be better than the

conventional organic matrices. This is significant as it facilitates analyte absorption and desorption processes, thus resulting in an improvement on spectra acquisition especially in the low mass range.[40]

In hyphenated techniques, the use of ICP-MS as a detector confers significant advantages. Specifically, it provides elemental stoichiometry and qualitative elemental information to control the recoveries and efficiencies in the synthesis of NPs. Size exclusion chromatography inductively coupled mass spectrometry (SEC-ICP-MS) is one such technique that has been used to obtain size distribution of AuNPs. HDC, an emerging alternative to SEC, has a short analysis time and requires minimal sample treatment. HDC-ICP-MS has been used for the characterization of Au and AgNPs.[36]

Another hyphenated technique is FFF-ICP-MS, which is considered highly versatile for the separation, detection, and quantification of NPs in real environmental matrices. FFF separates nanoparticles according to their hydrodynamic diameter in the absence of a stationary phase. FFF is the only technique that can fractionate NPs within the range of 1 to 100 nm. The technique can be coupled to different online detectors and can be operated under different pH and ionic strength conditions. Recently FFF-ICP-MS has been used for size characterization and mass determination of Ag and Au NP in aqueous media as illustrated by Bednar et al.[41] Mitrano et al. has compared two MS-based hyphenated approaches for the characterization of size distribution.[42]

Presently, the only technique currently capable of determining particle size distribution in addition to number and mass concentration for ENP-containing samples at or below 10 μg/L is SP-ICP-MS.[43] This interesting has been developed by Degueldre et al.,[43] and further method refinement has continued.[42,44−46] If samples containing NPs are introduced at a low flow rate and the number of particles in the solution is sufficiently low, analysis using ICP-MS in time-resolved mode makes it possible to collect the intensity for a single particle as it is vaporized and atomized in the plasma. Then, each measured data point can be correlated to the size and mass fraction of a unique NP. This method of NP characterization is called single particle ICP-MS (SP-ICP-MS) analysis. The key feature of this technique lies in the capacity of the ICP-MS to distinguish the data collected for each individual NP. Also, the different behaviors of the dissolved metal and metal NPs such as Ag and Au under single particle detection conditions have been used to differentiate directly between both forms of silver/gold in aqueous samples.[44] For this reason, care must be taken in the sample dilution (particle number in solution) and in the selection of the integration time.[41,42,44,47] Although the integration times used in the literature vary (typically around 5 ms), a maximum integration time of 10 ms is recommended[42,44,45,47] to avoid the double-counting highlighted above.

Jani et al. have investigated the particle size and concentration of silver nanoparticles within the range of about 20−80 using sp-ICP-MS.[43] Also, Laborda et al. have demonstrated that SP-ICP-MS can be used to differentiate between dissolved silver and silver nanoparticles in a sample. They achieved number concentration limits of detection of 1×10^4 L^{-1}[44]. Gray et al. extracted Ag and Au nanoparticles from biological matrices and used sp-ICP-MS to determine size distributions and particle number concentrations.[41]

The main drawback of the SP-ICP-MS technique is the size limit of ENP identification, currently approximately 20 nm for Au and Ag ENPs, which depends on the sensitivity of the instrument and the ionic background for the metal of interest.[44,46,48] Another challenge for SP-ICP-MS analysis is the application of the method to real samples and the use of this method to measure nanoparticles containing elements such as titanium, iron, or silicon due to the potential for spectral interferences.[49] Moreover, SP-ICP-MS is not suitable for determining the size of NPs (unless their elemental composition is previously known) because it is not able to distinguish between different particles with the same elemental composition. To overcome this limitation, a previous HDC separation was recently coupled online with SP-ICP-MS and applied to the simultaneous determination of the size, number concentration, and metal content of Au NPs.[50]

In summary, MS-based techniques have been shown to have a greater analytical application for the characterization of NPs as they may overcome drawbacks of better established techniques such as TEM/SEM, DLS, XPS, and UV−vis spectroscopy. In the future, MS-based techniques will be widely used for the characterization of water-soluble NPs and NP bioconjugate architectures.[51]

Electrochemical Characterization Using Nanostructured Poly(amic) Acid Membranes: A Case Study. The author's group has discovered that a new class of amphiphilic conducting poly(amic) acid (PAA) could be used to fabricate nanoporous membranes with potential applications in the filtration and detection of ENPs.[52−57] PAA is a conducting electroactive polymer, and its properties can be tuned by manipulating the delocalized π electron system for chemical and electrocatalytic applications. Its synthesis and molecular structure are given in Scheme 1. The carbonyl and amide functionalities in PAA act as anchors that have been previously employed in the fabrication of flexible nanostructured PAA−silica (PSG) films.[53]

We have reported the preparation of different classes of PAA membranes by keeping the processing temperature at or below 75 °C in order to avoid the imidization process in Scheme 1.[52,53,55−57] The low temperature prevented the cyclization of the PAA to polyimide, while retaining the intrinsic structural integrity and stability of the PAA. Depending on the composition, solvent used, and processing conditions, we have also discovered that PAA can be prepared as transparent stand-alone or translucent membranes, electrodeposited films on solid electrodes, and as permeable membranes for nanofiltration (Scheme 1).

The focus of this work is to utilize the specific transport and electronic conductivity of PAA membranes for filtration and detection of ENPs. When prepared using a phase-inverted process, PAA membranes have similar morphology as the typical phase-inverted membranes, which are thin, smooth, dense, and supported by a porous sublayer.[52,53]

The phase-inverted PAA derivatives were also found to have a number of unusual but practically favorable properties, in particular, a near-zero shrinkage or volumetric expansion upon curing (polymerization) as well as low water absorption. In addition, the polymers had high glass-transition temperatures as a result of their high cross-link densities. Explanations for these properties have been hypothesized in terms of favorable hydrogen-bonding effects, a sensitive ring current associated with aromatic moieties, and the ability of the PAA functional units to self-assemble into reversible polymeric networks. The smooth hydrophobic surfaces of the membranes lead to frictionless flow of water across the surface, thus enabling the

Scheme 1. Synthesis and Molecular Structure of Poly(Amic) Acid and Inhibition of Imidization Steps at Low Temperature for Electrodeposition, Stand-Alone Membrane Formation, and Nanoporous Membranes for Filtration and Sensing[a]

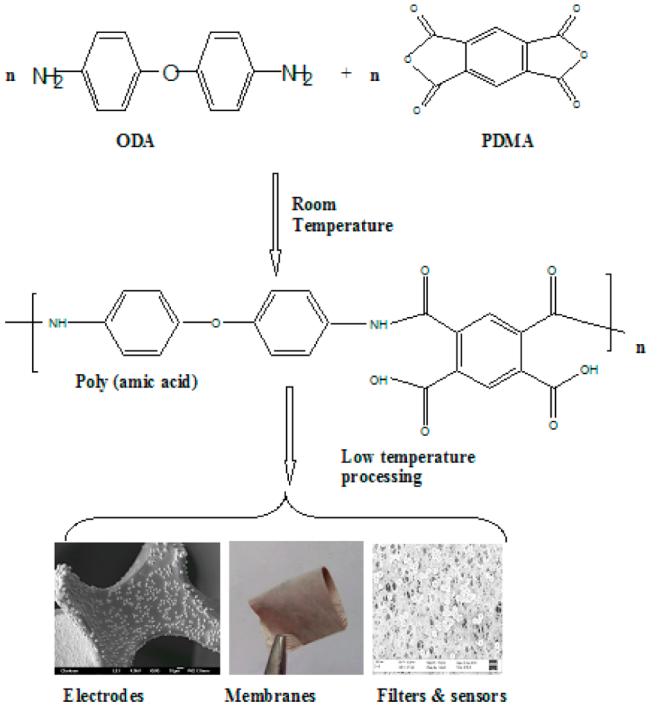

[a]PMDA = pyromellitic dianhydride, oxy-dianiline.

transport that is an order of magnitude higher than the transport in conventional pores. Figure 4 shows the SEM data obtained for PAA membranes using different concentrations of PAA solution. This synthetic approach affords well-controlled membranes, leading to various desired sizes (from less than 5 nm to greater than 100 nm).

Previous work using the PAA membranes for filtration of quantum dots, TiO_2, Fe_2O_3, and gold nanoparticles showed greater than 98% filtration efficiency. The present work demonstrates that the membranes could be retrofitted into a conventional tangential flow filtration mechanism for nanofiltration and electrochemical detection of silver nanoparticles.

Electrochemical Tangential Flow Filtration (EC-TFF). The design of a portable EC-TFF is shown in Figure 5. The portable analyzer contains nanostructured poly(amic) acid filter membrane electrode (PMFE) arrays incorporated within cassette filter, TFF analyzer, potentiostat, and reader.

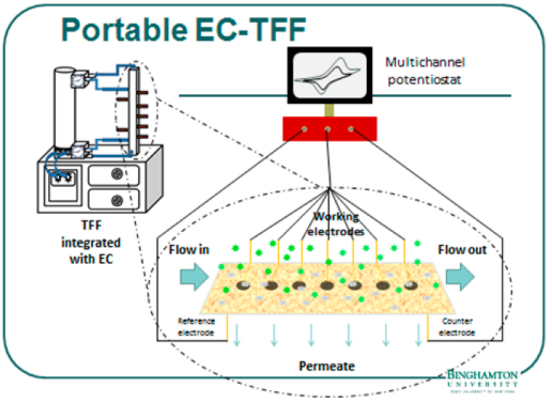

Figure 5. Design of the portable electrochemical tangential flow filtration system.

In EC-TFF, the sample solution is propelled by pressure initiated by a pump. As the feed enters the channel equipped with the PMFE membrane, molecules (e.g., ions) that are small enough to fit into the pores or macro voids of the membrane pass on the film as filtrate (permeate). All particles (e.g., bacterial, viruses, natural organic matter (NOM)) too large to fit through the pores are recycled back to the sample reservoir (retentate), and the cycle repeats. The application of electrical potential to the PMFE provides the added advantage of being able to detect the permeate downfield. The abundant carbonyl and amine group on the membrane act as "molecular anchors" to bind ENPs and isolate the particles. The porosity of the PMFE determines the molecular weight cutoff for both the permeate and the retentate. We ensured good retention by designing the PMFE that is 3−5 times size of the target molecule. Different classes of PAA membranes have been designed. One class was designed to retain particles in the range from 0.2−2 μm in width or diameter and up to 1−10 μm in length. These should be adequate for the nonspherical species including bacteria, viruses, and natural organic matter (NOM) varying from 200−60,000 amu/Da. Another class of PMFE membranes was designed for ENPs such as TiO_2, AgNP, and AuNP. The design of the PMFE array is shown in Figure 6. Electrode arrays were fabricated directly onto the PAA membranes (with the reference and counter electrodes fabricated onto the PAA membrane cassette).

Due to the widespread use of gold working electrodes, it was sputtered with gold film onto the lower side of the PAA membrane. The film thickness was tailored (by controlling the sputtering conditions) to ensure a favorable electrochemical response without blocking the pores of the PAA. Eight working electrodes were fabricated on one side of the paper substrate,

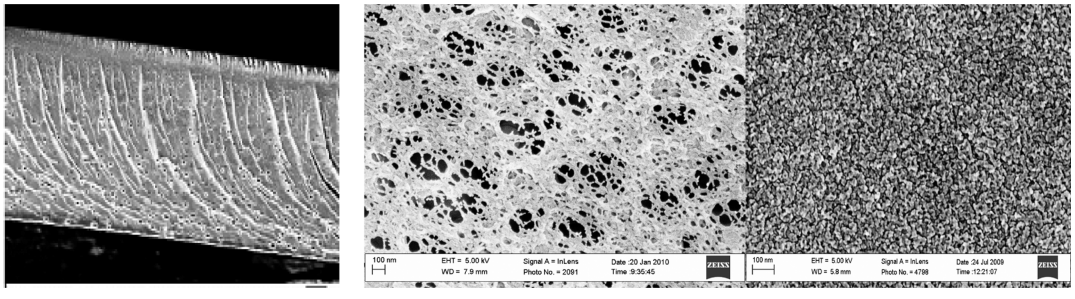

Figure 4. SEM of PAA membranes of varying pore sizes (left, cross section), middle (10−100), right (5−15 nm).

dx.doi.org/10.1021/sc500175v | ACS Sustainable Chem. Eng. 2014, 2, 1707−1716

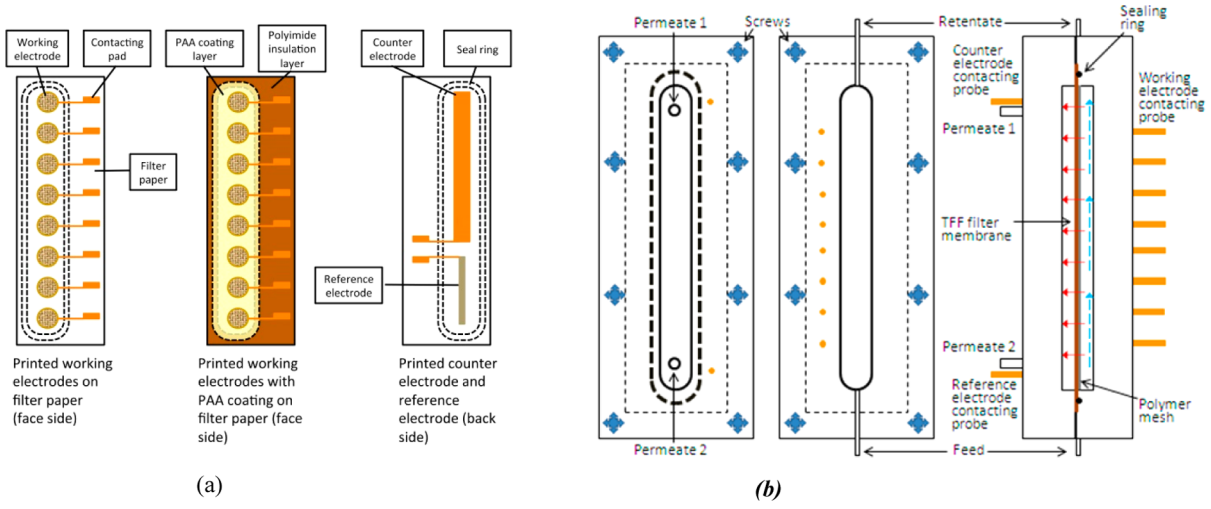

Figure 6. (a) Design of on-membrane electrode/filter combination. (b) Design of combined cassette/PAA membrane filter electrode for fluidic control.

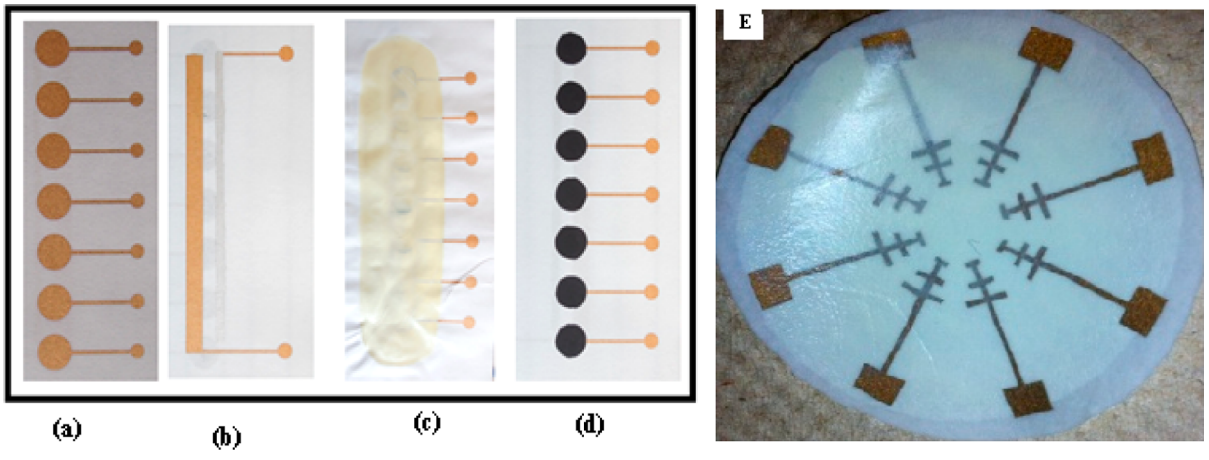

Figure 7. Sample PAA on-membrane electrodes: (a) Gold working electrodes on paper substrates, (b) gold counter and silver/silver chloride electrodes, (c) working electrodes coated with PAA membranes, and (d) carbon working electrodes. Right: Gold array electrodes fabricated onto paper substrates, with subsequent coating of PAA membranes (notice the shiny PAA).

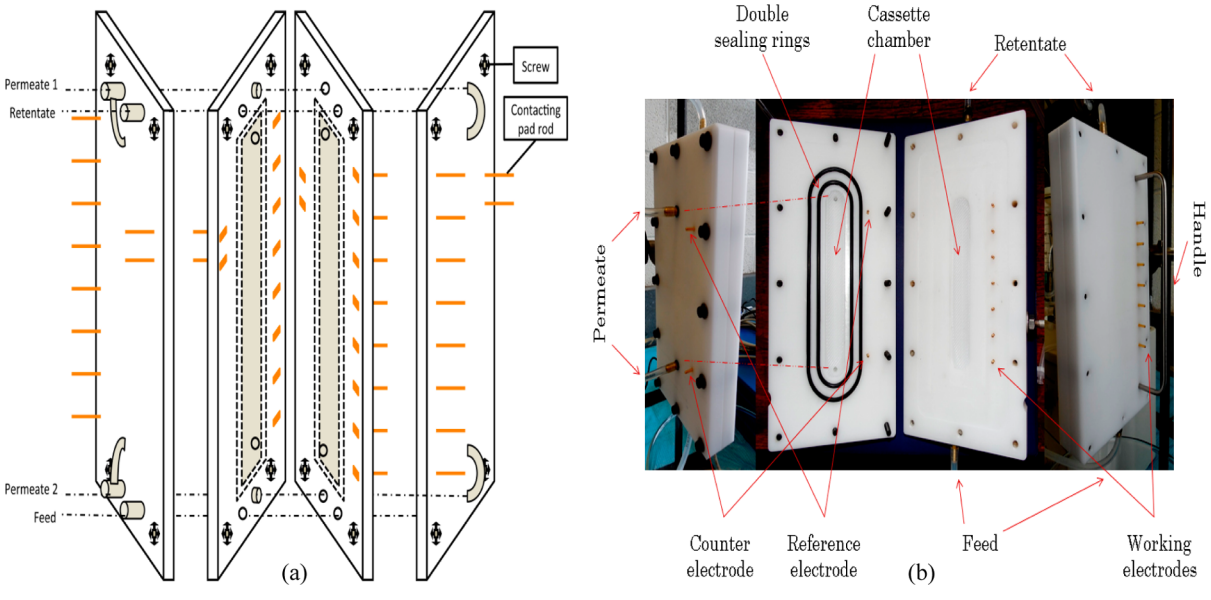

Figure 8. Design of integrated PMFE and prototype cassette for EC-TFF: (a) Cassette design and (b) production version of the cassette.

dx.doi.org/10.1021/sc500175v | ACS Sustainable Chem. Eng. 2014, 2, 1707−1716

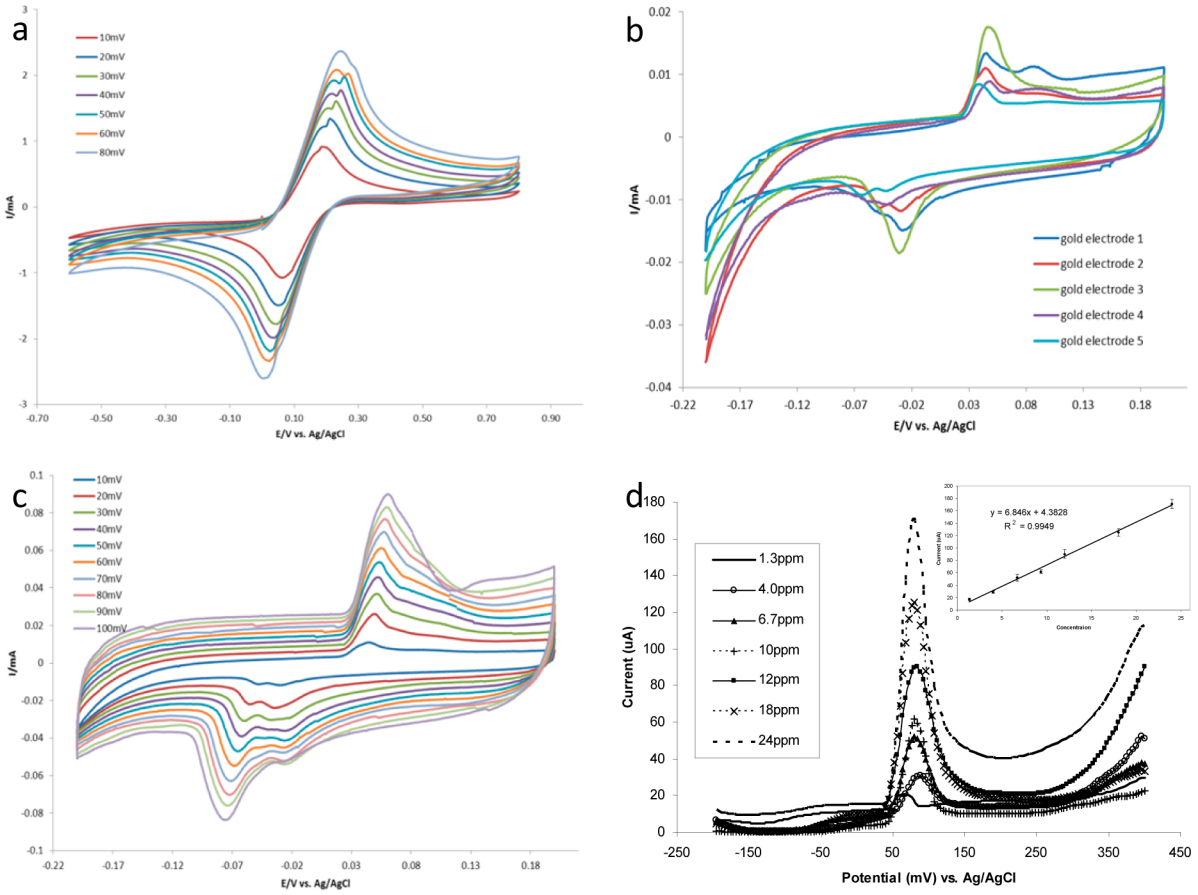

Figure 9. EC-TFF data for simultaneous electrochemical detection of nanosilver. (a) 10 mM K_3FeCN_6 in 0.1 M phosphate buffer solution as the supporting electrolyte,various scan rate on one of gold electrodes. (b) Silver NPs were detected on five gold electrodes in a parallel testing in 10 mM phosphate buffer with 0.25 M NaCl adjusted to pH 7.0 at a scan rate of 10 mV/s. (c) Silver NPs were detected on one of the gold electrodes at various scan rate in same buffer solution as b. (d) DPV data recorded for nanosilver in food supplements samples after filtration. DPV spectrum of standard 40 nm silver NPs at various concentrations. Experimental condition for DPV: 20 mV/s scan rate, 17 ms sample width, 50 ms pulse width, 200 ms pulse period, and 1 mA/V sensitivity. Experimental condition for CV: 50 mV/s scan rate and 100 μA/V sensitivity.

while the gold counter electrode and Ag/AgCl reference electrode were fabricated on the other side of the substrate. The surface of the working electrodes was covered by the PAA membrane to control the size of the filtered samples. Both sides of the filter paper outside the electrodes area (circled area in the center of filter paper) were insulated with polyimide. Figure 6b shows the design of the cassette to hold the PMFE. One piece (left) has the outlets for permeates and probes for counter and reference electrodes. The PMFE was placed into this piece, facing the other piece of the cassette as indicated by dashed rectangle lines. Then the sealing ring was placed on top of the PMFE as shown with the dashed circle ring. The other piece of the cassette (middle) has the outlets for feed and retentate and eight probes for working electrodes. The polymer mesh was placed in this piece to provide flow path. The right side of Figure 6b shows the flow direction for both main flow and cross-flow.

Figure 7 shows the actual PMFE electrode fabricated onto paper substrate. The electrochemical character of the cassette and PAA membrane were preserved simultaneously by controlling the electrochemical properties of the material surrounding the cartridge both on the diameter and on the ends. In addition, the cassette design provided sufficient structural support to accommodate routine handling. Figure 8 shows the design of the PAA electrode/membrane holder with electrodes. Eight working electrodes were fabricated on one side of the filter, while the gold counter electrode and Ag/AgCl reference electrode were placed on the other side of the filter. The surface of the working electrodes was modified with PAA membranes to control the size of the filtered samples. Both sides of the circled area in the center of filter paper were insulated with polyimide.

Figure 8 shows the design of the integrated PMFE and TFF process. One piece (left) has the outlets for permeates and probes for counter and reference electrodes. The PMFE was placed into this piece by facing the other piece of the cassette as indicated by dashed rectangle line. Then O-ring seal was placed on the membrane as indicated by the dashed circle. The other piece of the cassette (middle) has the outlets for feed and retentate. Eight probes were designed for working electrodes. The polymer mesh was placed in this piece to provide flow path. The right side of Figure 8 shows the direction of flow for both the main flow and cross-flow. A production version of this device was injection-molded and shown in Figure 8b. The electrochemical properties of the PMFE fitted onto the cartridge were tested using electrochemical techniques.

Electrochemical Characterization. In order to confirm that the gold electrodes fabricated onto filter paper are electrochemically active, we carried out cyclic voltammetry of ferricyanide. Cyclic voltammetry is often used to characterize

dx.doi.org/10.1021/sc500175v | ACS Sustainable Chem. Eng. 2014, 2, 1707−1716

conducting polymer films for studying the reversibility of electron transfer because the oxidation and reduction can be monitored in the form of a current−potential diagram. The electrochemical characterization of $K_3[Fe(CN)_6]$ of the bare gold array electrode surfaces was achieved by cycling the potential repeatedly between −600 and 600 mV at a varying scan rate between 10 and 100 mV/s. PMFE was then characterized in 0.1 M KCl at different scan rates (0.01−0.1 V/s). The oxidation and reduction peaks increased with the scan rates, which indicates a diffusion controlled reaction. In both tests using bare electrodes (carbon or gold) and a PAA-coated electrode, the redox peaks of $K_3[Fe(CN)_6]$ were observed (Figure 9). However, the bare carbon electrode gave a higher redox potential at 220 mV, while the PAA-covered electrode gave a redox potential at 190 mV.

When characterized in a supporting electrolyte, the PMFE showed two major peaks. The first redox couple (Epa1 and Epc1) referred to as $E^0$1, and the second redox couple (Epa2 and Epc2) referred to as $E^0$2. The PAA film was considered to have good diffusion-controlled electron mobility as evidenced by the increase in current response at both couples ($E^0$1 and $E^0$2) as the scan rate was increased. Randles Sevcik plots of current (A) vs scan rate (mV/s) confirmed a direct proportionality with correlation coefficients (R^2) of ±0.99. The peak where peak potential remains relatively constant for PAA indicates that the polymer film is attached onto the gold surface. The diffusion coefficient (D_e), which is a measure of how fast charge can be transported through the polymer layer, was calculated using Randles Sevcik equation

$$i_p = (2.68 \times 10^5)(n)^{3/2}(\mathrm{A})D_e^{1/2}(\mathrm{C})(v)^{1/2} \quad (1)$$

The D_e was found to be 7.10×10^{-6} cm^2/s for $E^0$1 and 9.11×10^{-6} cm^2/s for $E^0$2, in good agreement with the D_e of PAA previously reported.[51] After several hours, the top contacting pad area was still dry, which meant the PI insulation layer worked successfully.

EC-TFF for Characterization of Nanosilver. The EC-TFF designed was tested for the characterization of engineered nanosilver in food samples. Silver nanoparticles food supplement samples were purchased from various sources including mesosilver (>20 ppm) from Purest Colloids, Inc. (U.S.A.), colloidal silver (35−45 ppm) from Golden Touch Mfg./Ultra Pure (U.S.A.), and sovereign silver (10 ppm) from Natural Immunogenics Corp. (U.S.A.). The 40 nm AgNPs standard aqueous solution (Ted Pella, Inc.) was diluted with nanopure water in various concentrations. These solutions were used as AgNPs standards for electrochemical measurements. The efficiency of the PAA membrane for silver NPs was calibrated using the mesosilver sample. Mesosilver was mixed with deionized water into a series of diluted samples with different percentage concentrations (from 5% to 80%) compared to its original concentration (100%). The filtrate from the PAA membrane was measured, and concentration was compared with its original concentration.

The filtration or capture efficiency is defined as the percentage of NPs captured on the filter. Because the volume of sample is not changed before and after filtration, concentration was used instead of direct NPs number. Equation 2 shows the filtration efficiency (or capture efficiency) based on the change of NPs number and their concentration. Where η is filtration efficiency, N is number of NPs, and C is concentration.

$$\eta = \frac{N(\mathrm{captured})}{N(\mathrm{total})} \times 100\% = \frac{C(\mathrm{captured})}{C(\mathrm{total})} \times 100\% = \frac{C(\mathrm{total} - C(\mathrm{filtrate})}{C(\mathrm{total})} \times 100\% \quad (2)$$

Following the capture of the nanoparticles, simultaneous detection was achieved using differential pulse voltammetry. Nanosilver metal particles were thoroughly oxidized to metal ions using the applied electrical potential. Results show that there was no electrochemical signal recorded either for the blank electrode or the neat PAA membranes. However, upon coating the membranes with the nanoparticles, the redox peak was observed at ∼100 mV and was linearly dependent on the concentration of the silver nanoparticles (Figure 9d).

The differential pulse voltammetry (DPV) technique was also used to monitor the electrochemical oxidation of silver NPs following their isolation from food supplements samples. DPV has higher sensitivity than CV and could provide a better resolution as well as quantitative information related to trace amounts of silver NPs concentrations. Results showed that food supplement samples produced oxidation peaks at approximately the same potential (Figure 9d), while the control surfaces consisting of the blank gold and blank PAA membrane did not produce any peak in the range from −200 mV to 400 mV. In addition, the DPV of these food supplements not only produced the expected sharp oxidation peaks for the silver NPs but also showed some tailing after each peak. This can be attributed to transition of different oxidation states of silver oxides. Because the heights of these DPV peaks represented the amount of silver NPs in each samples, the concentrations of these food supplements samples were calculated from the calibration plots.

CONCLUSIONS

We have provided a short review of conventional and emerging techniques that are currently being used to characterize engineered nanoparticles. The challenges of microscopy (TEM, SEM, HRTEM, DLS, SNOM), chromatography (HDC, FFF), mass spectroscopy (ICP-MS, SEC-ICP/MS, MALDI, FFF-ICP-MS), sp-ICP-MS, and electrochemical techniques have been discussed. We have provided a case study for the design and fabrication of a new tool for ENP characterization based on EC-TFF. The EC-TFF method using PAA membranes was successfully used to capture and detect silver NPs quantitatively. The PAA membranes provided a simple approach to concentrate and isolate the NPs sample by varying filtration volume with minimal sample preparation, and the electrochemical detection was fast, requiring only few minutes. A conventional optical method can provide quantitative measurement only for nonprotected silver NPs, while an electrochemical method without PAA membranes cannot eliminate the effect of silver ions.

AUTHOR INFORMATION

Corresponding Author

*E-mail: osadik@binghamton.edu. Fax: 607:777-4478.

Notes

The authors declare no competing financial interest.

■ ACKNOWLEDGMENTS

The authors acknowledge the National Science Foundation, CBET 1230189, for funding.

■ REFERENCES

(1) Abe, S. Towards a standard vocabulary for nanomaterials relative to regulatory science. *Genes Environ.* **2011**, *33*, 10−13.
(2) Klaine, S. J.; et al. Nanomaterials in the environment: Behavior, fate, bioavailability, and effects. *Environ. Toxicol. Chem.* **2008**, *27*, 1825−1851.
(3) Tourinho, P. S.; et al. Metal-based nanoparticles in soil: Fate, behavior, and effects on soil invertebrates. *Environ. Toxicol. Chem.* **2012**, *31*, 1679−1692.
(4) Nowack, B.; Bucheli, T. D. Occurrence, behavior and effects of nanoparticles in the environment. *Environ. Pollut.* **2007**, *150*, 5−22.
(5) Handy, R. D.; et al. Practical considerations for conducting ecotoxicity test methods with manufactured nanomaterials: what have we learnt so far? *Ecotoxicology* **2012**, *21*, 933−972.
(6) Hull, M.; Kennedy, A. J.; Detzel, C.; Vikesland, P.; Chappell, M. Moving beyond mass: The unmet need to consider dose metrics in environmental nanotoxicology studies. *Environ. Sci. Technol.* **2012**, *46*, 10881−10882.
(7) Sadik, O.; et al. Sensors as tools for quantitation, nanotoxicity and nanomonitoring assessment of engineered nanomaterials. *J. Environ. Monit.* **2009**, *11*, 1782−1800.
(8) Richman, E. K.; Hutchison, J. E. The nanomaterial characterization bottleneck. *ACS Nano* **2009**, *3*, 2441−2446.
(9) Adams, F.; Van Vaeck, L.; Barrett, R. Advanced analytical techniques: platform for nano materials science. *Spectrochim. Acta, Part B* **2005**, *60*, 13−26.
(10) Rao, C.; Biswas, K. Characterization of nanomaterials by physical methods. *Annu. Rev. Anal. Chem.* **2009**, *2*, 435−462.
(11) Baer, D. R.; Gaspar, D. J.; Nachimuthu, P.; Techane, S. D.; Castner, D. G. Application of surface chemical analysis tools for characterization of nanoparticles. *Anal. Bioanal. Chem.* **2010**, *396*, 983−1002.
(12) Weinberg, H.; Galyean, A.; Leopold, M. Evaluating engineered nanoparticles in natural waters. *TrAC, Trends Anal. Chem.* **2011**, *30*, 72−83.
(13) Tiede, K.; et al. Detection and characterization of engineered nanoparticles in food and the environment. *Food Addit. Contam.* **2008**, *25*, 795−821.
(14) Liu, J.-f.; Yu, S.-j.; Yin, Y.-g.; Chao, J.-b. Methods for separation, identification, characterization and quantification of silver nanoparticles. *TrAC, Trends Anal. Chem.* **2012**, *33*, 95−106.
(15) Zenobi, R. Analytical tools for the nano world. *Anal. Bioanal. Chem.* **2008**, *390*, 215−221.
(16) Ahmed, T.; Imdad, S.; Ashraf, S.; Butt, N. M. Effect of size and surface ligands of silver (Ag) nanoparticles on waterborne bacteria. *Int. J. Theor. Appl. Nanotechnol.* **2012**, *1*, 111−116.
(17) Lankoff, A.; et al. The effect of agglomeration state of silver and titanium dioxide nanoparticles on cellular response of HepG2, A549 and THP-1 cells. *Toxicol. Lett.* **2012**, *208*, 197−213.
(18) Hassellöv, M.; Readman, J. W.; Ranville, J. F.; Tiede, K. Nanoparticle analysis and characterization methodologies in environmental risk assessment of engineered nanoparticles. *Ecotoxicology* **2008**, *17*, 344−361.
(19) Calzolai, L.; Gilliland, D.; Rossi, F. Measuring nanoparticles size distribution in food and consumer products: A review. *Food Addit. Contam., Part A* **2012**, *29*, 1183−1193.
(20) Wei, L.; et al. Investigation of the cytotoxicity mechanism of silver nanoparticles in vitro. *Biomed. Mater.* **2010**, *5*, 044103.
(21) Singh, R. P.; Ramarao, P. Cellular uptake, intracellular trafficking and cytotoxicity of silver nanoparticles. *Toxicol. Lett.* **2012**, *213*, 249−259.
(22) Lan, X.; et al. Magnificent CdS three-dimensional nanostructure arrays: The synthesis of a novel nanostructure family for nanotechnology. *CrystEngComm* **2011**, *13*, 145−152.
(23) Huang, X.; et al. Freestanding palladium nanosheets with plasmonic and catalytic properties. *Nat. Nanotechnol.* **2010**, *6*, 28−32.
(24) Jia, X.; Campos-Delgado, J.; Terrones, M.; Meunier, V.; Dresselhaus, M. S. Graphene edges: A review of their fabrication and characterization. *Nanoscale* **2011**, *3*, 86−95.
(25) Powers, K. W.; et al. Research strategies for safety evaluation of nanomaterials. Part VI. Characterization of nanoscale particles for toxicological evaluation. *Toxicol. Sci.* **2006**, *90*, 296−303.
(26) de Jonge, N.; Ross, F. M. Electron microscopy of specimens in liquid. *Nat. Nanotechnol.* **2011**, *6*, 695−704.
(27) Römer, I.; et al. The critical importance of defined media conditions in *Daphnia magna* nanotoxicity studies. *Toxicol. Lett.* **2013**, *223*, 103−108.
(28) Hecht, B.; et al. Scanning near-field optical microscopy with aperture probes: Fundamentals and applications. *J. Chem. Phys.* **2000**, *112*, 7761−7774.
(29) Pohl, D.; Denk, W.; Lanz, M. Optical stethoscopy: Image recording with resolution $\lambda/20$. *Appl. Phys. Lett.* **1984**, *44*, 651−653.
(30) Kaegi, R.; et al. Size, number and chemical composition of nanosized particles in drinking water determined by analytical microscopy and LIBD. *Water Res.* **2008**, *42*, 2778−2786.
(31) Fernández, B.; Costa, J. M.; Pereiro, R.; Sanz-Medel, A. Inorganic mass spectrometry as a tool for characterisation at the nanoscale. *Anal. Bioanal. Chem.* **2010**, *396*, 15−29.
(32) Bustos, A. R. M.; Encinar, J. R.; Fernández-Argüelles, M. T.; Costa-Fernández, J. M.; Sanz-Medel, A. Elemental mass spectrometry: A powerful tool for an accurate characterisation at elemental level of quantum dots. *Chem. Commun.* **2009**, 3107−3109.
(33) Jiang, X. Nanomaterials in analytical atomic spectrometry. *TrAC, Trends Anal. Chem.* **2012**, *39*, 38−59.
(34) Xie, H.; Huang, K.; Nie, X.; Tang, Y. Quantification of trace amounts of impurities in high purity cobalt by high resolution inductively coupled plasma mass spectrometry. *Rare Met.* **2007**, *26*, 286−291.
(35) Kokura, S.; et al. Silver nanoparticles as a safe preservative for use in cosmetics. *Nanomedicine* **2010**, *6*, 570−574.
(36) Tiede, K.; et al. Application of hydrodynamic chromatography-ICP-MS to investigate the fate of silver nanoparticles in activated sludge. *J. Anal. At. Spectrom.* **2010**, *25*, 1149−1154.
(37) Bustos, A. R. M.; Encinar, J. R.; Sanz-Medel, A. Mass spectrometry for the characterisation of nanoparticles. *Anal. Bioanal. Chem.* **2013**, 1−7.
(38) Wang, L.; et al. Monodispersed core-shell Fe_3O_4@ Au nanoparticles. *J. Phys. Chem. B* **2005**, *109*, 21593−21601.
(39) Fontes, A. et al. Quantum Dots in Biomedical Research. In *Biomedical Engineering—Technical Applications in Medicine*, 1st ed.; Hudak, R., et al., Eds.; InTech: Rijeka, Croatia, 2012; pp 269−290.
(40) Rainer, M.; Qureshi, M. N.; Bonn, G. K. Matrix-free and material-enhanced laser desorption/ionization mass spectrometry for the analysis of low molecular weight compounds. *Anal. Bioanal. Chem.* **2011**, *400*, 2281−2288.
(41) Gray, E. P.; et al. Extraction and analysis of silver and gold nanoparticles from biological tissues using single particle inductively coupled plasma mass spectrometry. *Environ. Sci. Technol.* **2013**, *47*, 14315−14323.
(42) Mitrano, D. M.; et al. Silver nanoparticle characterization using single particle ICP-MS (SP-ICP-MS) and asymmetrical flow field flow fractionation ICP-MS (AF4-ICP-MS). *J. Anal. At. Spectrom.* **2012**, *27*, 1131−1142.
(43) Degueldre, C.; Favarger, P.-Y.; Bitea, C. Zirconia colloid analysis by single particle inductively coupled plasma−mass spectrometry. *Anal. Chim. Acta* **2004**, *518*, 137−142.
(44) Laborda, F.; Jiménez-Lamana, J.; Bolea, E.; Castillo, J. R. Selective identification, characterization and determination of dissolved silver (I) and silver nanoparticles based on single particle detection by inductively coupled plasma mass spectrometry. *J. Anal. At. Spectrom.* **2011**, *26*, 1362−1371.
(45) Pace, H. E.; et al. Single particle inductively coupled plasma-mass spectrometry: A performance evaluation and method comparison

in the determination of nanoparticle size. *Environ. Sci. Technol.* **2012**, *46*, 12272−12280.
(46) Pace, H. E.; et al. Determining transport efficiency for the purpose of counting and sizing nanoparticles via single particle inductively coupled plasma mass spectrometry. *Anal. Chem.* **2011**, *83*, 9361−9369.
(47) Tuoriniemi, J.; Cornelis, G.; Hassellöv, M. Size discrimination and detection capabilities of single-particle ICPMS for environmental analysis of silver nanoparticles. *Anal. Chem.* **2012**, *84*, 3965−3972.
(48) Von der Kammer, F.; et al. Analysis of engineered nanomaterials in complex matrices (environment and biota): General considerations and conceptual case studies. *Environ. Toxicol. Chem.* **2012**, *31*, 32−49.
(49) Sannac, S.; Tadjiki, S.; Moldenhauer, E. *Single Particle Analysis Using the Agilent 7700x ICP-MS*; Application Note 5991-2929EN; Agilent Technologies, Inc.: Santa Clara, CA, 2013.
(50) Rakcheev, D.; Philippe, A.; Schaumann, G. E. Hydrodynamic chromatography coupled with single particle-inductively coupled plasma mass spectrometry for investigating nanoparticles agglomerates. *Anal. Chem.* **2013**, *85*, 10643−10647.
(51) Sapsford, K. E.; Tyner, K. M.; Dair, B. J.; Deschamps, J. R.; Medintz, I. L. Analyzing nanomaterial bioconjugates: A review of current and emerging purification and characterization techniques. *Analytical Chem.* **2011**, *83*, 4453−4488.
(52) Andreescu, D.; Wanekaya, A. K.; Sadik, O. A.; Wang, J. Nanostructured polyamic acid membranes as novel electrode materials. *Langmuir* **2005**, *21*, 6891−6899.
(53) Du, N.; et al. Flexible poly (amic acid) conducting polymers: effect of chemical composition on structural, electrochemical, and mechanical properties. *Langmuir* **2010**, *26*, 14194−14202.
(54) Omole, M. A.; et al. Catalytic reduction of hexavalent chromium using flexible nanostructured poly (amic acids). *ACS Catal.* **2011**, *1*, 139−146.
(55) Omole, M. A.; K'Owino, I. O.; Sadik, O. A. Palladium nanoparticles for catalytic reduction of Cr (VI) using formic acid. *Appl. Catal., B* **2007**, *76*, 158−167.
(56) Noah, N. M.; et al. Conducting polyamic acid membranes for sensing and site-directed immobilization of proteins. *Anal. Biochem.* **2012**, *428*, 54−63.
(57) Hess, E. H.; Waryo, T.; Sadik, O. A.; Iwuoha, E. I.; Baker, P. G. Constitution of novel polyamic acid/polypyrrole composite films by in-situ electropolymerization. *Electrochim. Acta* **2014**, *128*, 439−447.